RECONSTRUCTING THE LITTLE ICE AGE GLACIAL RETREAT USING DENDROGLACIOLOGY IN CENTRAL TIAN SHAN MOUNTAINS, CHINA

by

Elizabeth M. Schumann, B.S., M.S.

A thesis submitted to the Graduate Council of
Texas State University in partial fulfillment
of the requirements for the degree of
Master of Science
with a Major in Geography
August 2022

Committee Members:

Yanan Li, Chair

Nathan Allen Currit

Samantha Marie Krause

FAIR USE AND AUTHOR'S PERMISSION STATEMENT

DEDICATION

To my husband Shayne.

ACKNOWLEDGEMENTS

My thesis would not have been possible without the help of my advisor, my professors, and all my friends and family. Thank you Dr. Yanan Li for taking me on as your student, and for offering me your help and guidance on this project. Thanks also to the members of my graduate committee, Dr. Nathan Currit, and Dr. Samantha Krause, for their advice and recommendations on my thesis. Thank you as well to Mrs. Allison Glass-Smith for all of her help navigating the required paperwork and coursework.

I thank Texas State University, including the Graduate School, and the Department of Geography and Environmental Studies. Thank you to Aidan McLendon for your help and advice as a fellow student, and for some fun lunches. Thank you to Kate Landers, who mounted and sanded all the tree core samples, preparing them for analysis.

Also, thank you to my father, Bryan Schumann, my sister Miriam McCurley and my grandparents, Linda, and Richard Schumann, for their love and support throughout my time here at Texas State University. Thank you to my husband, Shayne O'Brien for his love, help and support while I worked through the many drafts of my thesis.

TABLE OF CONTENTS

LIST OF TABLES

Table **Page**

LIST OF FIGURES

Figure **Page**

ABSTRACT

Glaciers are sensitive indicators of the changing climate, and quantitative constraints on the timing of past glacial events provide key information in climate models. This thesis uses dendroglaciological techniques to reconstruct the age of the terminal moraine in the forefield of the Xiata Glacier, located in the central Tian Shan Mountains in Northwest China. This study aims to answer the following two research questions: What is the timing of the most recent Little Ice Age glacial retreat event in the area? And how does the timing of the central Tian Shan's Little Ice Age (LIA) glacial event correspond to other LIA events in High Mountain Asia?

A series of 48 core samples taken from 35 trees growing on the outer flanks of the Xiata glacial moraine were collected in the summers of 2017 and 2019 and used to inference the moraine age after lab processing and age correction. Taking considerations of germination date and the ecological succession of trees on the moraine, results suggest that the most recent moraine-forming retreat of the Xiata Glacier occurred around 1547 A.D. and potentially 1810 A.D, during the LIA. These results fit well with known Little Ice Age cold periods in Northwestern China and are similar to ages found at other sites within High Mountain Asia, particularly the Southeastern Tibetan Plateau. Additionally, this study compares two laboratory methods to examine if semi-automatic image analysis is more efficient than the traditional manual operation when measuring tree ring width series. The former is found cheaper and less time-consuming, suggesting a potentially more accessible option for students and researchers without sacrificing measurement

accuracy.

The findings from this study help fill in the knowledge gap in this remote region and helps provides additional context to other LIA studies in HMA. Tree-ring data is a powerful tool that offers insight into the timing of past glacial movements and yields key information in climate change research.

1. INTRODUCTION

1.1 Overview

Glaciers are sensitive indicators of the changing climate (Schickhoff, Singh, and Mal, 2016; Shean et al., 2020; IPCC, 2021). Various aspects of glacier change (e.g. changes in length, area, mass, and volume) can be used to determine changes in climate (Schickhoff, Singh, and Mal, 2016). Over the past two decades, studies have recognized a global trend of increasing ice loss and glacial retreat (Schickhoff, Singh, and Mal, 2016; Shean et al., 2020), with few glaciers experiencing advance (Fujita and Nuimura, 2011; Rankl, Keinholz, and Braun, 2014; Schickhoff, Singh, and Mal, 2016). Most of such studies are relying on the remotely sensed data which are only available to the most recent several decades. Natural proxies, such as tree rings, lake sediments, glacial deposits and dating techniques associated can help a better understanding of past glaciers and climate changes in a centennial, millennial, or even longer temporal context.

Understanding current and past glacial fluctuations is essential to establishing how glaciers respond to climate change. This information is vital for adaptation strategies to mitigate glacial meltwater replenishment for downstream communities and for predicting natural disasters, such as glacial lake outbursts and mudslides (Wang et al., 2013; Yang et al., 2021).

Globally, numerous studies have examined glacial fluctuation with the aid of tree ring proxy data, including in Chile (e.g. Warren and Sugden, 1993; Harrison and Winchester, 2000; Koch and Kilian, 2005), the Canadian Rockies (e.g. Luckman and Osborn, 1979; Luckman, 1994), British Columbia, Canada (e.g. Lewis and Smith, 2004), and in Scandinavia (e.g. Karlén, 1984). Tree rings have become a preferred proxy for estimating the timing of glacial retreats when glacial depositional features, such as lateral or terminal moraines, avail this type of data material. Many of these dendroglaciology studies, however, concentrate on glaciers in North and South America and across Europe (e.g. Luckman, 1994; Wiles et al., 1999; Koch and Kilian, 2005). The region of High Mountain Asia (HMA) has been historically neglected, and contemporary studies are beginning to fill in this gap in recent decades (e.g. Rankl, Kienholz, and Braun, 2014; Maurer et al., 2019; Farinotti et al., 2020; Yang et al., 2021). The existing literature has been primarily focused on the Tibetan Plateau, the Himalayas, and the central Karakoram (e.g. Bräuning, 2006; Fujita and Nuimura, 2011; Miller, Immerzeel, and Rees, 2012; Xu et al., 2012; Zhu et al., 2013; Xu and Yi, 2014; Hochreuther et al., 2015; Maurer et al., 2019; Zhu et al., 2019; Farinotti et al., 2020; Yang et al., 2021) and lacks dendroglaciology research in other potential sites on the periphery of the HMA, for example, the Tian Shan mountains in Central Asia.

To date, very few studies have utilized the central Tian Shan region for climate change research. This represents a substantial gap in knowledge. The Tian Shan Mountain range spans 2,500 km and is uniquely positioned between the four countries of Uzbekistan, Kyrgyzstan, China, and Kazakhstan. Meltwater from the Tian Shan glaciers feed into many rivers (e.g. Tarim River, Ili River, and Syr Darya River) and their tributaries throughout the region, providing a critical source of freshwater for oases and villages downstream, and is a critical factor for agricultural and socioeconomic development (Li and Fu, 2019). Given the importance of the glaciers within this region, knowing how glaciers have changed and its relation to climate is paramount as climate change brings forth new challenges to these glacier-fed, vulnerable, yet under-studied regions.

In this study, the Xiata Glacier in the Harajoriha Range (5400 m. a.s.l.) of the central Tian Shan (CTS), within the Xinjiang Uyghur Autonomous Region of northwestern China will be investigated using dendroglaciological analysis to determine the timing of the most recent glacial retreat. I will measure samples using two methods (manual vs. semi-automatic) to evaluate the discrepancy in accuracy and efficiency. The goal is to quantitatively assess the advantages and disadvantages of each method. The application of dendroglaciology in the Xiata Glacier valley will be the first such case study of the CTS. The new data and knowledge generated from this study will help us better understand the timing of a specific glacial event and its (dis)agreement to the regional and global climate background. The results of this work will be prepared for publication in a peer reviewed academic journal.

1.2 Purpose Statement

The purpose of this study is to approximate the timing of the Little Ice Age (LIA) glacier retreat in the central Tian Shan (CTS) range. The established dendroglaciology method of tree ring analysis will be used alongside available remotely sensed data of the region.

Trees along the outer flank of the terminal moraine will be cored and analyzed to determine the age of the oldest tree. This information will help estimate the minimum formation age of the terminal moraine. This minimum moraine age can then be used to estimate the timing of the most recent LIA glacial retreat in the study area. This research will add to the body of knowledge for the timing of glacial fluctuations within the CTS. These findings will also be compared to contemporary studies throughout the Tian Shan and nearby regions to determine the synchronicity of the glacial event at a larger spatial context.

In addition, two tree ring analysis methods (manual and semi-automatic) will be used and compared for accuracy and efficiency. The traditional method of manually measuring tree rings in a core sample with the aid of a microscope will be compared to the newer semi-automatic method of using specialized computer software and high-resolution photo analysis. The findings from this methodological aspect will provide a better understanding of the time and cost associated with each method given the accuracy of the measurements is not sacrificed.

1.3 Research Questions

This research aims to determine the timing of LIA glacial events in the CTS. By using dendroglaciology this research will answer the following questions:

1. What is the timing of the most recent Little Ice Age glacial retreat event in the central Tian Shan Mountains?

2. How does the timing of the central Tian Shan mountains Little Ice Age glacial retreat event correspond to other LIA glacial retreat events in High Mountain Asia?

From a methodological perspective, this study will utilize manual and semi-automatic tree ring measuring methods to answer the following questions:

1. Is there a statistical difference between the ages produced by the two methods?

2. If no statistical difference exists in results, which of the two methods is more efficient in terms of time and cost?

1.4 Conceptual Framework

Tree-ring dating principles are applied to assign ages to glacial landforms primarily through two approaches. One method utilizes trees that have been damaged or killed by advancing glaciers. The outermost rings of these killed or damaged trees ‘mark’ the year that the glacier advanced to that position (Speer, 2010). The second method ages trees that have recolonized the glacial landform to determine the age of the formation and inference the timing of glacial retreat (Sigafoos and Hendricks, 1969; Smith and Lewis, 2007). This study will use this second method to inference the timing of glacial retreat in the CTS.

In areas that have been previously glaciated, moraines can offer important insight for paleoenvironmental reconstructions. As a glacier advances, it pushes the sediment and other surrounding materials ahead of it. After the glacier retreats, these pushed materials are left behind, forming a ridge composed of glacial till (unconsolidated and unsorted sediment). Therefore, this remaining ridge, known as a moraine, is indicative of past glacial movements. Depending on its location, formation process, and characteristics, glacial moraine contains a variety of types, such as terminal moraine, lateral moraine, recessional moraine, and hummocky moraine (Schomacker, 2011). Of interest to this study is the terminal moraine, which marks the furthest extent of the past glacier (Lewis, 1884).

After the formation of the moraine, trees may start to sprout on this freshly exposed surface, if permitted by the temperature and tree line of the ecosystem (Speer, 2010). Early work by Lawrence (1946), and subsequent researchers (e.g., McCarthy and Luckman, 1993; Osborn et al., 2007), established that the total number of annual rings from the trees that first begin to colonize the freshly exposed moraine provides a minimum estimate of surface age. By determining the oldest age of the colonizing trees, the inferred moraine age can provide a chronology of the most recent glacial histories

(Heusser, 1956; Smith et al., 1995; Luckman, 2000).

There are several factors to be considered when attempting to determine the age of a glacial moraine using tree core samples. Because it is not feasible to sample every tree growing on the moraine surface, the trees that are sampled need to be carefully selected. The best location to find the oldest trees is on the outer flank of the moraine due to the colonization process (Figure 1). Samples also need to be accurately dated to find the age of the oldest tree. In addition, the accuracy in determining moraine age can be affected by the ecesis interval (EI) and the germination date.

The ecesis interval (EI) is the lapse in time between the establishment of available surface for growth (stabilization) and seed germination on that surface (McCarthy and Luckman, 1993; Koch and Kilian, 2005; Zhu et al., 2013). The EI needs to be added to the oldest colonizing tree on the moraine surface to infer the stabilization date.

The process for determining the EI is not standardized and this interval can vary widely even for the same tree species because of local climate (McCarthy and Luckman, 1993). There are several methods that have been used in previous work to determine the EI. Studies have: 1) sampled seeds in plots of known or estimated ages to determine ecesis (Clements, 1904; Palmer and Miller, 1961; Oliver, Adams, and Zasoski, 1985); 2) sampled tree species appearing along several transects perpendicular to an ice front to obtain a measure of ecesis (Lutz, 1930); 3) calculated ecesis by subtracting the tree age from the number of years that the surface was known to have been exposed (Sigafoos and Hendricks (1969); and 4) compared the germination date with estimates of the date of moraine formation with the use of lichenometry (Burbank, 1981).

McCarthy and Luckman (1993) performed a comparative study, analyzing these past methods of ecesis determination, and found that the numerous assumptions required between these methods resulted in, "…a range of moraine dates that may be as broad as available ecesis estimates." They proposed that to obtain the most precise estimate for ecesis, the germination dates of trees growing on moraines should be compared to the dates from trees that were damaged or killed during glacial advance. The availability of such damaged or killed trees, however, are scarce to non-existent in most cases. Other methods have sought to determine the EI by comparing historical images to germination dates. Zhu et al. (2019), determined the EI for three tree species (*Hippophae tibetana, Pinus wallichiana,* and *Larix griffithii*) within the southern half of the Tibetan Plateau by finding the difference in the germination year of the oldest tree and historical images/records.

Germination is the development of a plant from a seed after a period of dormancy (Bewley and Black, 1994). The germination date of the oldest tree on the moraine provides the minimum estimate of the surface age, and thus, the minimum date for the glacier event (Sigafoos and Hendricks, 1969; McCarthy and Luckman, 1993; Smith and Lewis, 2007). By adding the determined EI and germination date to the age of the oldest tree, the best approximation can be achieved for the timing of the most recent LIA glacial retreat.

The ideal approach for determining the germination date is by counting the annual rings in a cross section that has been taken from the root crown (germination) level. However, this approach is not practical, because it is destructive sampling, which is often not permitted, and it is extremely difficult to reach the root crown level for sampling due to sediment or other obstacles in the way (McCarthy, Luckman, and Kelly, 1991). A modification to this method is to sample within the first ≤ 20 cm of the tree trunk to help ensure that the germination tissues are collected (Zhu et al., 2019). For samples taken above 20 cm, the mean height growth rate is calculated to determine the sample height age to ensure the most accurate age possible is assigned. When the pith of the tree is missed during coring, the pith offset needs to be calculated to determine the true age of the tree. The method to determine the pith offset for this project is discussed in further detail in section 4.3, but it can also be calculated by using the Geometric method by Duncan (1989), or by using pith indicators (Applequist, 1958).

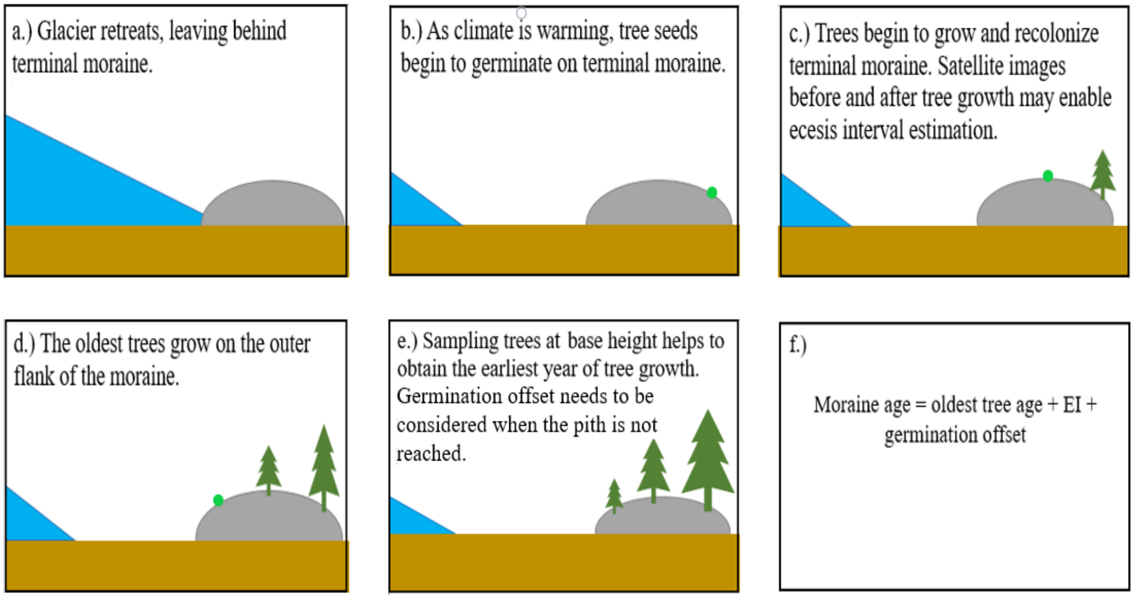

Figure 1. Conceptual framework depicting formation of the terminal moraine, and colonization of trees on the glacial landform.

2. LITERATURE REVIEW

2.1 Climate Change and Glaciers

Glaciers are an established indicator of climate change (Bertrand et al., 2012; Harrison, 2013; Schickhoff, Singh, and Mal, 2016; Shean et al., 2020). The most recent report from the Intergovernmental Panel on Climate Change (IPCC AR6, 2021), states that between 2010 and 2019, glaciers have had more mass loss than in any other time since the start of observational records. Between 1993 and 2010, inland glacier mass loss contributed more to sea level rise (0.86 mm year $^{-1}$) than the ice sheets (0.60 mm year $^{-1}$) (IPCC, 2013). Glacier ice loss contributed 22% to sea level rise between 1971 and 2018 (IPCC, 2021). Mountain glaciers are now recognized to have a more rapid response to climatic drivers, such as temperature and precipitation, than ice sheets (Oerlemans, and Fortuin, 1992; Roe, Baker, and Herla; 2017 Maurer et al., 2019).

Surface air temperature and precipitation in the Tian Shan Mountains have been increasing between 1960 and 2016, with various studies finding similar results (Wang et al., 2011; Wang et al., 2013; Xu et al., 2018). Temperature has increased by 0.33°C per decade, even though the rest of China has only experienced an increase of 0.22°C per decade (Wang et al., 2011; Xu et al., 2018). This increase in surface temperature has been specified as the main driver in the 11.5% decrease of total glacial area since 1960 in the Tian Shan Mountains (Wang et al., 2011).

Precipitation is also an important driving factor for glacier mass balance, although it has been shown to have more regional variability (Wang et al., 2011; Wang et al., 2013; Xu et al., 2018). The eastern TS has seen a decrease in precipitation between 1960 and 2016, averaging 2.64 mm per decade, while western portions have seen an increase averaging 8.07 mm per decade during the same period (Wang et al., 2013; Xu et al., 2018). The overall amount of precipitation throughout the Tian Shan Mountains has increased between 5.82 mm to 11 mm per decade since 1960 (Wang et al., 2011; Xu et al., 2018).

This rise in temperature and precipitation poses a hazard to downstream communities that rely on the steady supply of glacial meltwater throughout the year. The ramifications of glacier loss have been seen in communities in other areas (Miller, Immerzeel, and Rees, 2012; Sidgel et al., 2020); thus, it is important to understand how glaciers within the CTS have fluctuated in the past, to better predict how they will respond in the future to continued climate change.

2.2 The Little Ice Age

The term 'Little Ice Age' (LIA) was first published in 1939 (Matthes, 1939). This concept once broadly considered the LIA to be the most recent 4,000-year climatic interval (Late Holocene) and was in reference to cooling trends in Europe and North America, associated with several glacial advances and retreats (Mann, 2002). Today, the LIA is defined as the period of cooling that occurred approximately between 1300 and 1860 (Mann, 2002; Grove, 2004; Matthews and Briffa, 2005; Miller et al., 2012). Multiple studies determined that the LIA contains three cooling periods centered around 1650, 1770, and 1850 (NASA, 2021). Glacier advances have been reconstructed during the LIA period across the globe (IPCC, 2001), however, the periods of maximum glacial extent during the LIA vary considerably across regions, suggesting independent regional climatic changes (Bradley and Jones, 1993; Mann et al., 1999; IPCC, 2001; Mann, 2002).

Within HMA, the periods of cold from the LIA appear to be asynchronous. The Eastern Monsoon area of China may have been the first to experience effects of the LIA in the 1300s, with three pronounced cold periods in the 14th, 17th, and 19th centuries (Qian and Zhu, 2002). The Tibetan Plateau in western China did not appear to be affected by the LIA until between 1620 and 1749 with significant cold temperatures (X. Zhang et al., 2013). Zhu (1972) reported that the period between 1650 and 1700 was one of the coldest recorded in Chinese history. With respect to these cold events, the temperatures within eastern China are still considered relatively uniform between 1100 – 1800 (Mann, 2002).

2.3 Proxy Data

Climate proxies possess physical characteristics related to climate that stand in for direct meteorological measurements allowing for the reconstruction of past climatic conditions (Hawkins, 2020). These data are often relied upon in the study of past climates because of the lack of credible climate records, such as documentary records and thermometer measurements (Mann, 2002). Numerous kinds of proxy data have been developed using ice cores, pollen, and sediment cores, among others, to infer past climates.

Glaciers leave few direct records of retreat or mass loss, proxy sources, however, provide insight into climatic history for which observational data rarely exist, especially in regions that are understudied. Numerous proxies have been used to date glacial history and inference past climate. Some common methods are lichenometry, radiocarbon dating of organic matter, cosmogenic radionuclides (CRN) exposure dating, and dendroglaciology. Lichenometry, a dating method that uses lichen growth to determine the age of rock, can provide a quick age for an exposed surface, but is not a close estimate of true age, and can be subject to error (Osborn et al., 2015; McCarthy, 2002). Bickerton and Matthews (1992), determined that, even under ideal lichenometry conditions, only 10% of results were accurate at the LIA timescale. Radiocarbon dating and CRN exposure dating are two other common methods, but can be quite costly (Putkonen and Sawnson, 2003; Libby, 1963). Radiocarbon dating relies on the availability of organic matter which are rare in high glaciated elevations. CRN exposure dating utilizes cosmic ray induced radionuclides in rocks to determine age. Exotic boulders are commonly found in glacial landscapes, but laboratory processing procedures are complex and costly. Several studies have used these methods in the past decades within HMA and the Tian Shan (Solomina, Savoskul, and Cherkinsky, 1994; Yi et al., 2004; Kong, Fink, and Huang, 2009; Saha, Owen, and Caffee, 2019). Dendroglaciology uses tree rings to inference the age of the glacial surfaces. By dating rings from trees near the glacial terminus and previously glaciated areas as proxy data, a temporally refined reconstruction of the glacier's history can be revealed, allowing analysis of glacial movement in centennial timescales.

2.4 Dendrochronology and Dendroglaciology

The field of dendrochronology focuses on dating tree rings to the year that they originally formed (Fritts, 1976; Stokes and Smiley, 1996). Tree rings are an excellent proxy record because of their physiology and ease of collection. As trees grow rings annually, climatic records can be gleamed from counting and assessing the rings. For example, rings are typically wider during favorable conditions and will narrow during less favorable conditions (Figure 2). Signs of infections or damage (e.g. glacial advance, mudslides, or wildfires) are also ‘recorded’ by the rings, offering more insight to past events (Hawkins, 2020).

One of the earliest mentions of trees producing annual rings comes from Theophrastus in 332 BC (Studhalter, 1956). As far back as the 13th and 14th centuries, naturalists began to discern the annual character of tree rings and began searching the environment for the causes of change in tree ring growth (Speer, 2010). Leonardo da Vinci even recorded the annual growth of tree rings, suggesting that their growth was affected by the weather (Stallings, 1937; Sarton, 1954; Corona, 1986).

By the early 1990s, the technique of crossdating, developed by A. E. Douglas (Fritts, 1976), was used to determine the year that tree rings were formed (Speer, 2010). The process of crossdating consists of matching the patterns of wide and narrow rings in core samples so that each ring can be assigned to its year of formation (Figure 3). Samples are compared from within the same tree and between different trees to get as accurate a date as possible (Fritts, 1976). Since then, these dendrochronological techniques have been applied in many fields of studying climate and earth processes, such as dendroarchaeology, dendroclimatology, dendroecology, dendrogeomorphology, dendrochemistry, and dendroglaciology (Speer, 2010).

Dendroglaciology is the branch of dendrochronology that uses tree rings to study and date the movement of glaciers (Luckman, 1988; Schweingruber, 1988). One of the earliest uses of dendroglaciology dates to William Sherzer (1905), who used the growth of spruce trees to estimate the age of glacial moraines in the Canadian Rockies. Numerous studies have since used dendroglaciology to date glacial advance and retreat (e.g. Smith and Laroque, 1996; Wiles et al., 1999; Harrison and Winchester, 2000;

Lewis and Smith, 2004; Koch and Kilian, 2005; Bräuning, 2006; Koch, 2009; Xu et al. 2012; Hochreuther et al., 2015). One critical drawback of tree ring dating is that trees must grow in areas with distinct warm and cold seasons so that distinct rings can be formed between seasons and can be counted. Trees in tropical locations with year-round growth generally do not form rings, and are rarely used for dating purposes (Butler, 1987). Despite these difficulties, annual chronologies and climate response can be derived from trees in tropical areas (Anchukaitis, et al. 2012).

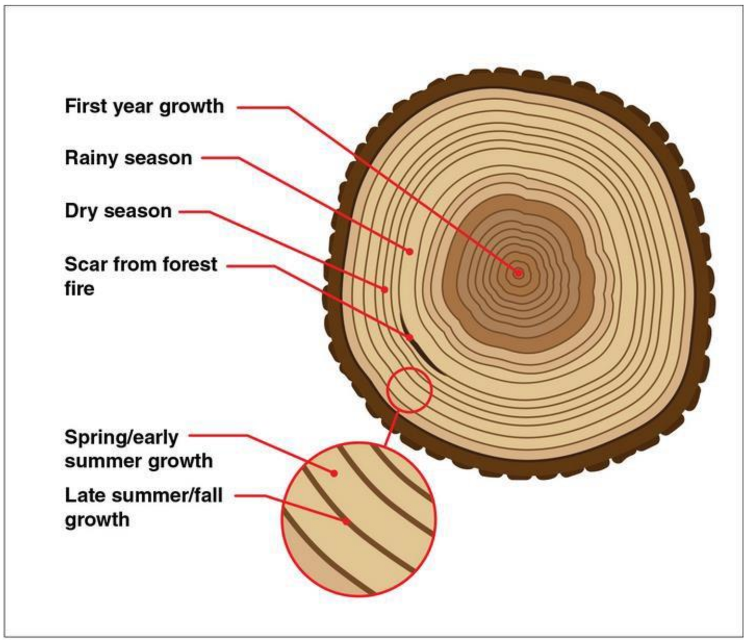

Figure 2. Tree ring growth response to environmental factors (Stoller-Conrad, 2017).

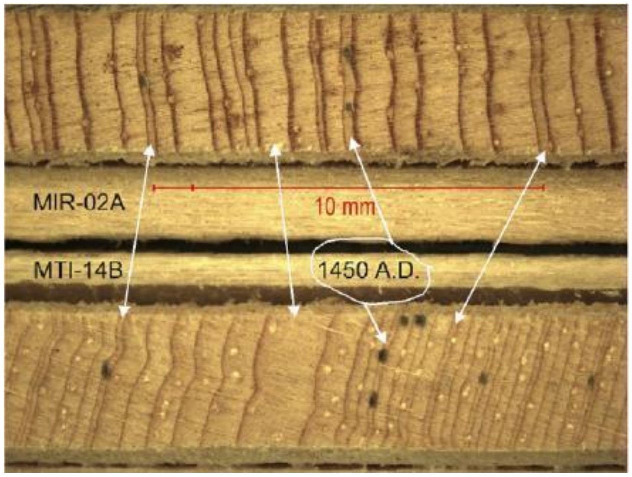

Figure 3. The process of crossdating tree cores to create a chronology (Biondi et al., 2011).

3. STUDY AREA

The Tian Shan (TS), located in Central Asia, is a major mountain range that spans ~2500km west-east across Tajikistan, Uzbekistan, Kyrgyzstan, China, and Kazakhstan. This vast range was formed from the uplift caused by the India-Asia collision, and is composed of several smaller ranges (Jolivet, et al., 2010; Li and Fu, 2019). The main ranges that constitute the central Tian Shan (CTS) are the Tomur, Khan-Tengri, and Haditor-Harajoriha Ranges. These three ranges have average altitudes of 6600 m, 6000m, and 5400 m above sea level (a.s.l.), respectively (Li et al., 2017; Li and Fu, 2019). The major atmospheric circulations that dominate the area are the westerlies, the Siberian high, and Asian monsoon. The total annual precipitation from 1981 to 2010 was 362.3 mm, and the average annual temperature was -6.7°C (Solenn, 2008).

Precipitation primarily occurs in the TS between May and September, and can be as much as 1,000 mm annually, decreasing at a rate of 30 mm per 100 m of decreased elevation (Jolivet et al., 2010; Li and Fu, 2019). Orographic blocking of westerly winds causes precipitation to be concentrated on the windward side of the mountains. The combined effect of these forces creates the ideal conditions for glaciers to form.

The Harajoriha Range is located within the Xinjiang Uyghur Autonomous Region of China, just northeast of Peak Tomur, the highest peak of the TS (Figure 4). A previous study by Li and Fu (2019), mapped a 489 km^2 section of this range, focusing on the watersheds of the Xiata River and the Muzart River. The Xiata Basin provides snow and ice meltwater for the Xiata River as it flows north. The largest glacier in the Xiata Basin is the Xiata Glacier, of which the proglacial area is the focus of this study (Figure 5). The 0.8 km^2 proglacial area, features the LIA terminal moraine that this study is attempting to date. The LIA moraine is located at an altitude of 2,720 m a.s.l, which is below the 2,900 m a.s.l. treeline (Li and Fu, 2019). The species of tree that is most commonly found growing on the terminal moraine surface is Schrenk Spruce (*Picea schrenkiana)*. These trees form distinct annual rings, making this an ideal location for using dendroglaciological techniques to determine the age of the moraine.

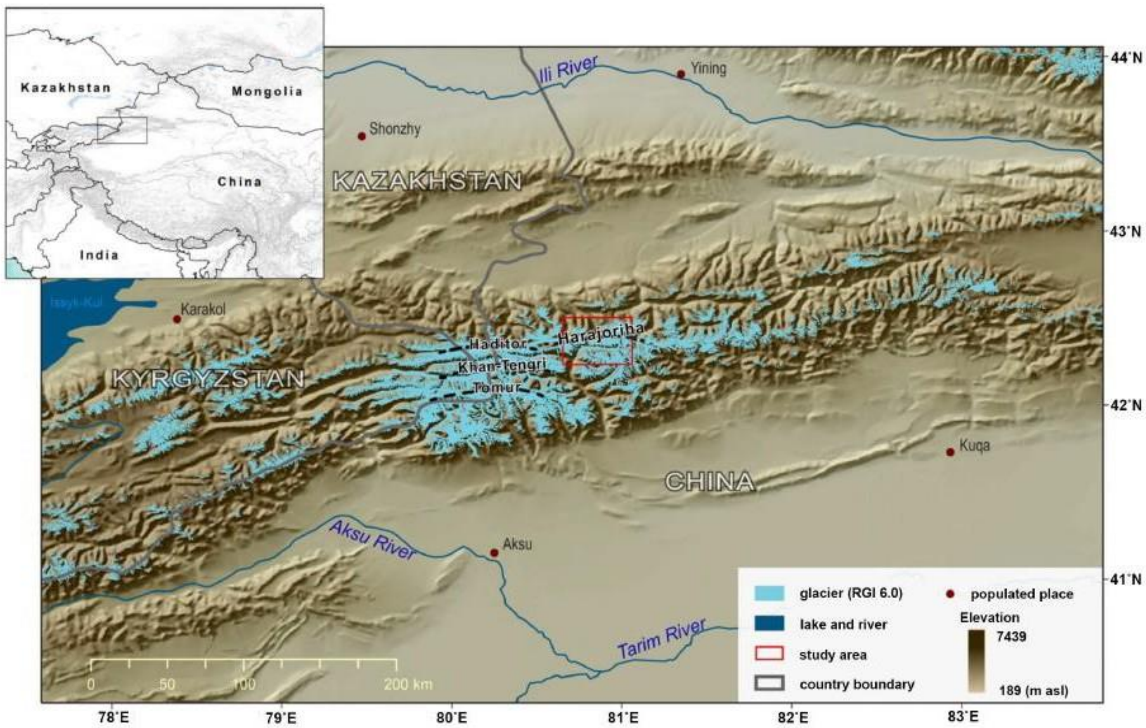

Figure 4. Regional setting of the mountain ranges in the CTS and the location of the study area in the Harajoriha Range (red box) (Li and Fu, 2019).

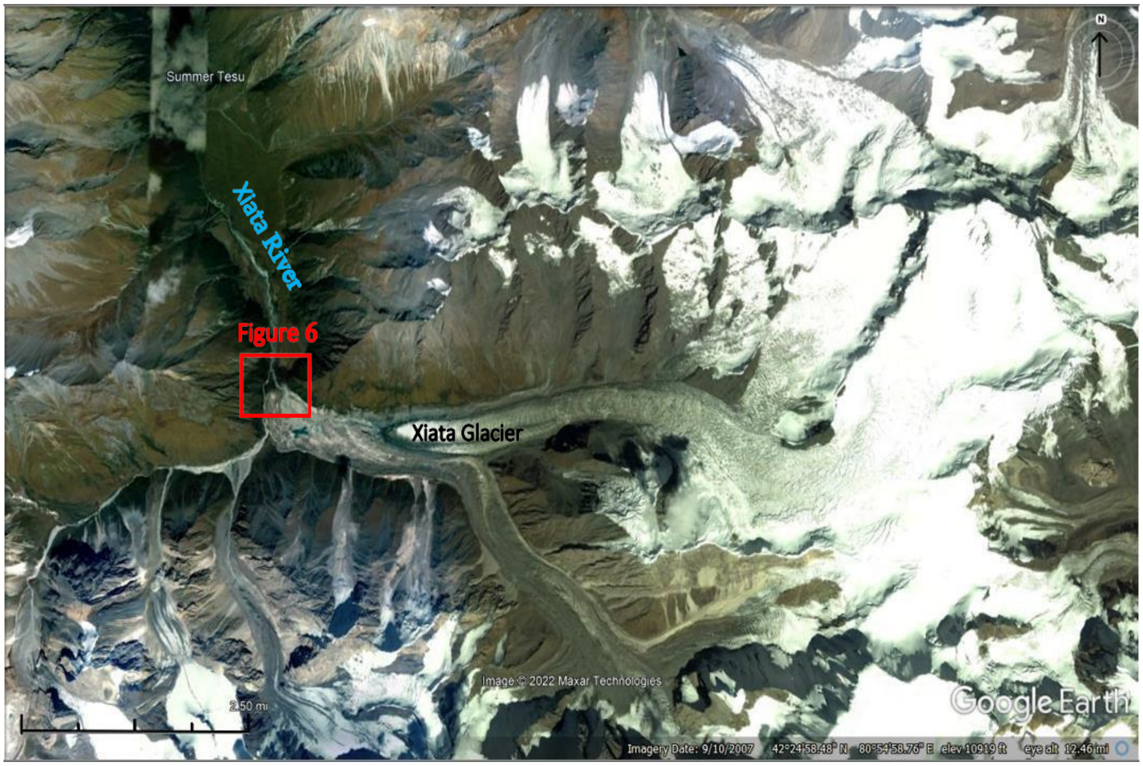

Figure 5. The proglacial area of the Xiata Glacier viewed on GoogleEarth. The red box indicates the specific study site illustrated by Figure 6.

4. METHODS

4.1 Field Methods

Site Selection

The study site represents a recently glaciated forefield and has numerous trees growing on the closest terminal moraine, assumed to be formed during the LIA. This setting provides the opportunity for dendrological analysis within this understudied region. The dominant tree species growing on the terminal moraine is *Picea schrenkiana* (Schrenk's spruce). This species is ideal for use in this study is known to grow seasonal rings in this alpine region (Butler, 1987; T. Zhang et al., 2013; Zhang et al., 2016; Huo et al., 2017). The trees to be cored were selected using targeted sampling. This is a common practice used within the field of dendrochronology to target areas where samples are known to exist, and to maximize the information that can be gathered with minimum resources. For this project, only trees that appeared to be the oldest in each sampling area were selected for coring. The topography, slope, aspect, hydrology, and tree density were considered when selecting the sampling sites due to their effects on the longevity of trees. The exact location of the trees sampled can be seen in Figure 6.

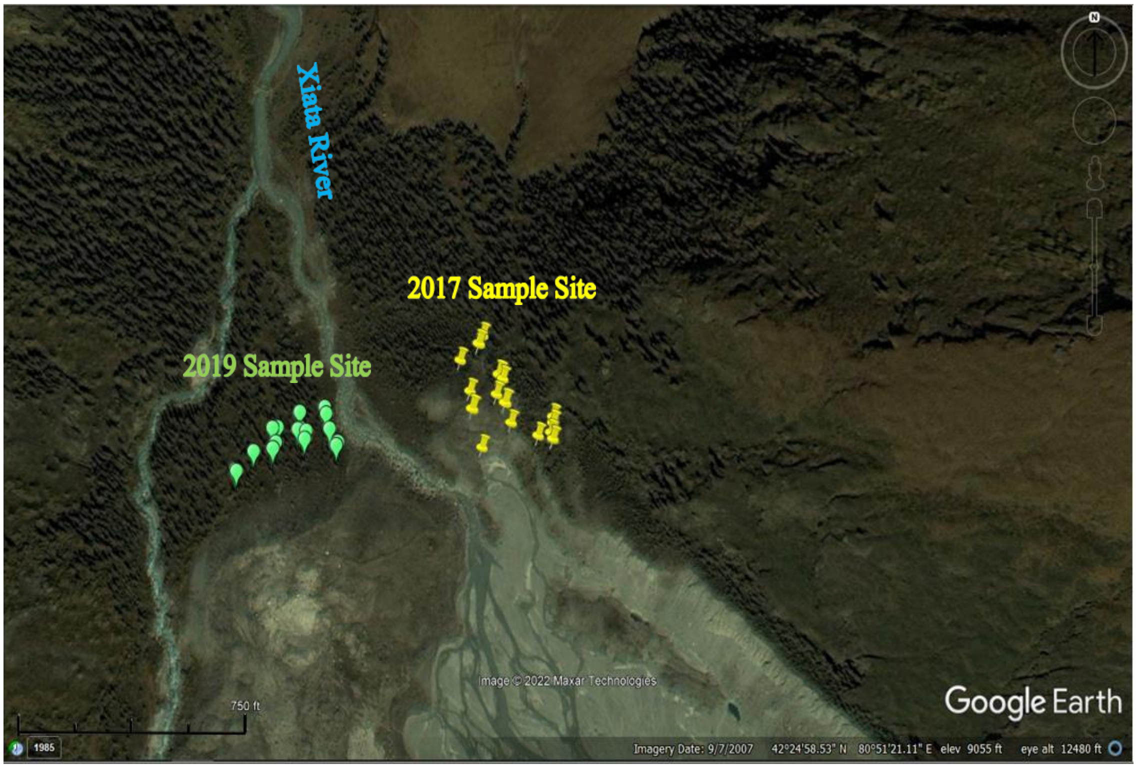

Figure 6. Location of the trees that were sampled on the terminal moraine surface. The yellow pins indicate trees that were cored in the summer of 2017, and the green pins indicated trees that were cored in the summer of 2019. Image captured from GoogleEarth.

Tree Core Collection

Tree core samples were taken from trees growing on the surface of the terminal moraine using an increment borer (Figure 7). A total of 37 trees were sampled (52 tree cores) during the 2017 and 2019 field seasons. The tree cores collected in 2017 were cored at breast heights, while trees in 2019 were sampled as close to the base of the tree as possible to ensure the inclusion of the germination year in the tree core sample (Zhu et al., 2019). Staying within the suggested 20 cm tree height was not always possible, due to the terrain (e.g., steep slope, presence of boulders). The sample height for each core can be seen in Table 1.

Core samples were placed into paper straws for protection and transport. The paper straws allowed the cores to dry without the risk of mold. Information such as the date, location, tree number, and core orientation were written on the straws as well as in a field notebook. The increment borer was carefully cleaned between each use to help maintain it and to prevent the potential spread of disease between individual trees.

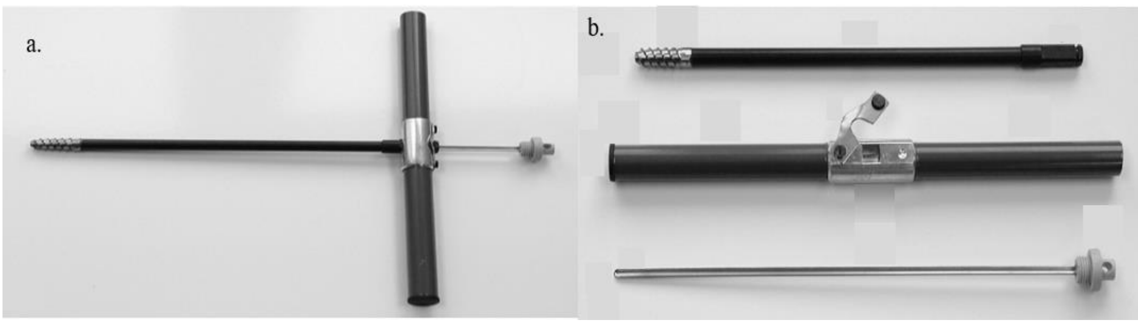

Figure 7. The increment borer showing: a.) the equipment assembled; b.) the equipment disassembled (Grissino-Meyer, 2003).

Table 1. Sampling height (cm) of tree core samples used in this study.

2017 Samples			2019 Samples		
Tree ID	**Core ID**	**Height (cm)**	**Tree ID**	**Core ID**	**Height (cm)**
XTN01	A	27	XTX01	A	40
XTN02	A	28		B	20
XTN03	A	77		C	20
XTN04	A	85	XTX02	A	48
XTN05	A	98		B	36
XTN06	A	67	XTX03	A	30
XTN07	A	53		B	49
XTN08	A	75	XTX04	A	28
XTN09	A	37		B	33
	B	37	XTX05	A	40
XTN10	A	56		B	30
XTN11	A	42	XTX06	A	38
XTN12	A	33		B	34
XTN13	A	23	XTX07	A	34
XTN14	A	35		B	26
XTN15	A	47	XTX08	A	35
XTN16	A	63		B	36
XTN17	A	55		C	38
XTN18	A	89	XTX09	A	28
XTN19	A	71		B	36
XTN20	A	78		C	25
			XTX11	A	33
				B	33
			XTX12	A	30
				B	30
			XTX13	A	30
				B	30
			XTX14	A	38
				B	38
			XTX15	A	29
				B	29
			XTX16	A	40
				B	20

4.2 Laboratory Methods

Pre-processing

Prior to measurement, core samples need to be prepared through several steps, including mounting, air drying, and sanding (Stokes and Smiley, 1968). The tree cores from the 2017 field season were previously processed and analyzed by collaborators from the Chinese Academy of Sciences.

Pre-processing was performed by past graduate student (2020), Kate Landers, who began by mounting and gluing the tree cores into a grooved wooden mount. Once the glue was dry, each core was sanded with progressively finer grade sandpaper until there was a smooth, polished finish with clearly visible ring patterns.

Tree-ring Measurement: Manual Method

For the manual analysis, each of the cores from 2019 was measured and dated using the Velmex Tree Ring Measuring System ("TA"). This system consists of the following:

- Main components:
    - UniSlide® dovetail rapid advance screw motion assembly
    - One micron (0.001 mm) resolution linear encoder integrated to the UniSlide assembly
    - Velmex VRO™ Encoder Readout for connection to the linear encoder and interface serially to a computer for measurement recording/logging
- Accessories:
    - VXM-USB to RS232 Serial Cable
    - VRO-TAB2 remote reset and send remote input module

The Velmex system was used in conjunction with a microscope and computer software. The microscope used was a stereo zoom microscope with a trinocular boom stand by AmScope. The software used to capture and edit the measurements was the MeasureJ2X developed by Project J2X. An additional eyepiece with crosshairs, and a ring LED light were purchased as well to help ensure that accurate measurements were being taken.

The tree cores were individually viewed through the microscope, on the UniSlide. A core was placed so that the outermost year, the year of collection, was the first ring to be measured. The vertical line of the crosshair in the eyepiece was then aligned so that it was perpendicular to the outermost edge of a ring, and the send button on the VRO-TAB2 remote was pressed. The remote and sliding micrometer were connected to the Velmex VRO Encoder Readout which displayed the current measurement in millimeters and sent it to the MeasureJ2X program on the computer.

This process was continued down the length of the core, until the pith (center) was reached. If the pith was not present, the rings were counted and measured until they began to curve inwards and form concentric rings. This inward curvature is indicative of the pith (Stokes and Smiley, 1968; Duncan, 1989; Speer, 2010).

After the measurements for each core was completed, a text file containing all the ring widths and their corresponding years was compiled and saved by using the MeasureJ2X software.

Tree-ring Measurement: Semi-automatic Method

For the semi-automatic method of analysis, each of the cores from 2019 were scanned and dated by using the high-resolution Espen Perfection V850 Pro Scanner and the program CooRecorder. All tree cores were scanned at a resolution of 2400 dpi. The tree cores were scanned in three batches, as the scanner is capable of scanning several cores at once, greatly reducing the time normally required to obtain such high-resolution images. It takes about 30 minutes for each batch scan. The resulting three images were each cropped so that only cores from the same tree were in a single image. Cropping the image also reduced the file size, since the originally scanning images were too large to be opened in CooRecorder.

The cropped images were opened in the CooRecorder program. This software is specifically designed for dating tree cores. Beginning with the outermost tree ring, an area was selected, and the program automatically placed markers in the selected area where it detects the boundary of a new tree ring. This process is only semi-automatic because the user is required to verify the identified tree ring boundaries for errors in identification. The program detects a tree ring by identifying the change in color between the lighter “earlywood” and darker “latewood.” As a result, the program may potentially misidentify scars, rot, false rings, and double rings as annual rings. When a misidentified ring is found, it can easily be deleted, and the program will automatically adjust the dates along the entire core. Prior to analyzing each core, the user inputs the year of the outermost ring, and the program counts backwards from this start point, and dates each successive ring measured.

4.3 Oldest Tree Age

Step 1: Crossdating

Crossdating for tree ring width measurements can be done by using a variety of programs, two of the most common being COFECHA and dplR, an R package. For this project, I used the dplR package, ran in the xDateR application (Bunn, 2008; Bunn, 2010) to analyze and assess the data. This method is preferred over running the code in R because the application immediately produces visuals, making it easier to detect any issues in dating. xDateR also allows for easy insertion or deletion of tree rings and updates the results in real-time. By doing so it is easy to examine the data for instances of false rings, frost rings, or missing rings. This function saves times and helps pinpoint which sections of poorly dated tree cores need to be re-examined.

Crossdating ensures that each tree is assigned its exact year of formation. This process is accomplished by matching the wide and narrow patterns of the tree rings between cores from the same tree, and between trees from the same location (Stokes and Smiley, 1968; Speer, 2010). The more trees used in creating the chronology, the more accurate it will be. The xDateR application compares the measurements from all the tree core samples and creates a chronology that it can then compare to each individual tree core.

The statistics that the application produces are the gini coefficient, the autoregression coefficient, and the series intercorrelation. These statistics show how well a tree ring series is crossdated. The gini coefficient is a measure of the equality of the value, ranging between 1 and 0. A value of 1 indicates that all the measurements are the same, and a value of 0 indicates that none of the measurements are similar. The autoregression coefficient (ar1) is a measure of how much the previous year's growth is affecting the current year's growth.

Finally, the series intercorrelation is a measurement of how well each tree core sample correlates to all the other cores samples. Each tree core is crossdated with all the other cores in the sample to compile a reference chronology for the area. CDendro (the partner program to CooRecorder) compares each individual core to the reference chronology and calculates a series intercorrelation value. Unusually high or low coefficients can be an indicator of improper dating and can signal the presence of false or absent rings. Numerous factors (e.g. site, precipitation, temperature, tree species) can affect how well trees correlate with each other. In general, a series intercorrelation above 0.40 can be considered reaching a reliable crossdating result.

Step 2: Pith Offset

One key factor that can offset the dating of a tree core is the pith. The pith is located at the center of the tree, and if it is reached when coring a tree, the tree can be dated to its exact age. If the pith is missed during coring, the pith offset, or the number of years missed, must be determined to obtain the trees exact age (Duncan, 1989; Speer, 2010). For this project, pith offset was determined by using the pith offset tool in the CooRecorder program (Figure 8). This process matches the curvature of a series of concentric rings to the curvature of the tree rings seen in the core sample. The size of the concentric rings used is based on the average tree ring size in the core sample. Once aligned, the number of rings that are missing can be counted, giving a rough estimate of the true pith date (Speer, 2010).

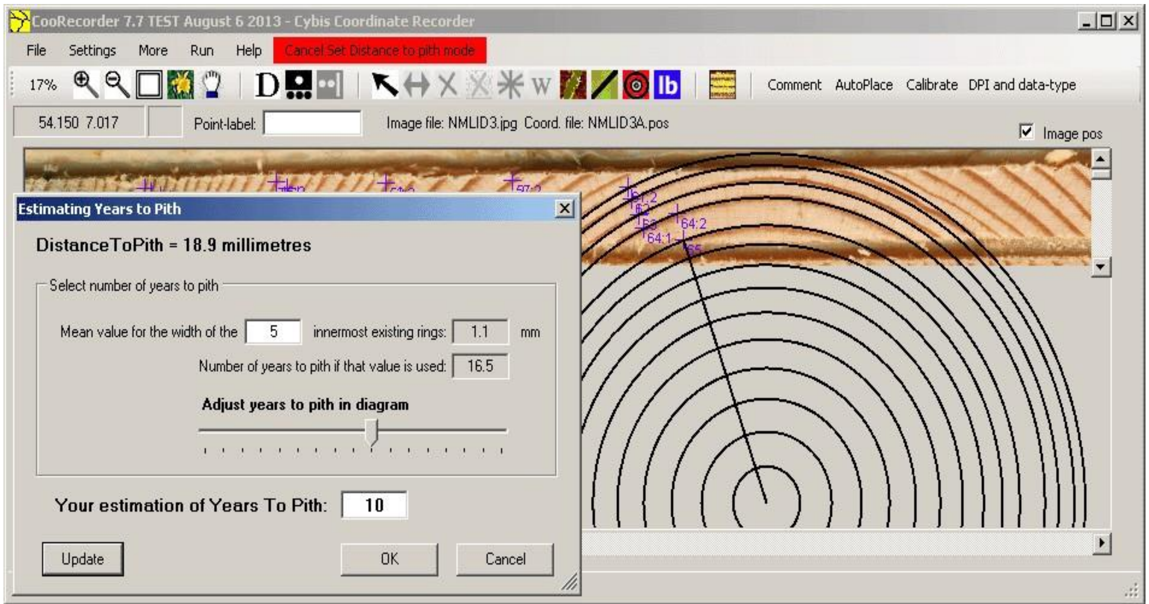

Figure 8: Screenshot from CooRecorder, demonstrating the how the pith offset tool counts the missing rings to the pith (Image by cybis.se).

Step 3: Germination Dates

Taking tree cores from the root collar, the portion of the root system that transitions into the stem, helps ensures that the oldest tissues of the tree are sampled, providing the oldest age of the tree (McCarthy, Luckman, and Kelly 1991; Telewksi, 1993). The root collar can be obscured by erosion or sedimentation, thus, requiring that the core sample be taken farther up the trunk (Telewski and Lynch, 1991; Telewski, 1993). A detailed record of the sample heights can be seen in Table 1.

The germination date (GD) for the 2017 trees was determined by using the same method as in Xu et. al (2012). Most of the trees cored in 2017 had only one sample taken, so the mean height-growth rate (HGR cm/year) was determined by using the 2019 samples. Cores were taken from multiple heights on the same tree, allowing for the estimation of the mean height-growth rate. To determine the sample height age, the sampling height (cm) was divided by the mean height-growth rate.

Finally, to determine the germination date, the height age was subtracted from the core pith year after curvature adjustment (Equation 1). The trees sampled in 2017 only had one core taken per tree, so the 2019 growth rate is applied because the tree species, climatic condition, and microenvironment are considered the same.

$$GD = P - \left(\frac{SH}{\left[\Sigma \frac{(SH_1 - SH_{2)}}{(SA_2 - SA_1)}\right]/n}\right)$$

Equation 1: Formula for determining the germination date (GD). The variables are explained by the following: Pith year (P), Sample Height (SH), Sample Age (SA), number of samples (n). Note: this calculation only considers when a lower SH_1 renders a bigger SA than a higher SH_2.

4.4 Estimation of Glacier Retreat

To accurately estimate glacier retreat, the ecesis interval (EI) needs to be determined. The EI is the lag time between ground surface stabilization (assumed to occur when the glacier retreats) and seedling germination (McCarthy and Luckman, 1993; Kurtz and Baker, 2016). For this project, satellite imagery was used to attempt to determine the EI. Satellite imagery of the study site was visually inspected for bare ground. If acceptable images were identified, subsequent images would be examined for the first appearance of trees over the same area. The temporal difference between these two images would then be the EI for the area. Due to the inaccessibility of high-resolution images for this remote area, the EI was unable to be determined using this method. Because of this, the suggested EI of 7 years by Passmore et al. (2008) was used. This is not the ideal method for determining the EI, however, because Passmore et al. (2008) was conducted on the same species, *P. schrenkiana*, within the Tian Shan, therefore provides a reliable EI for use in this study.

5. RESULTS

5.1 Evaluations on Manual and Semi-automatic Methods

Manual and Semi-automatic Ages

To determine if the ages obtained by the two methods were significantly different, a Wilcoxon signed rank test was used. This analysis was selected because the data were non-parametric as determined by the Shapiro-Wilk Test for Normality, and it is nonparametric equivalent to the Student's t-test. Results show that the tree ages obtained between the manual and semi-automatic methods were not significantly different. These ages were only determined for the 2019 samples, and results of ages using each method can be seen in Table 2. The average difference in the determined ages was 1.77 years, with tree XTX08 having a notable difference of 10 years between the two methods.

Table 2. Tree ages obtained from the manual and semi-automatic methods, and the difference in ages.

Tree ID	Manual Age	Semi-automatic Age	Age Difference
XTX01	203	203	0
XTX02	196	195	1
XTX03	110	112	2
XTX04	114	111	3
XTX05	139	140	1
XTX06	168	168	0
XTX07	129	130	1
XTX08	374	384	10
XTX09	189	189	0
XTX10	509	510	1
XTX11	163	167	4
XTX12	78	78	0
XTX13	97	97	0
XTX14	46	77	1
XTX15	151	150	1
XTX16	170	167	2
XTX17	378	381	3

Average Age	190.82	191.77	1.77

Manual and Semi-automatic Time and Cost

The efficiency of two experimented methods is evaluated based on the total time and cost consumed. Both methods were performed by the same person, thus no human errors are considered. The cost of each method was totaled from purchase receipts, and thus was easily and accurately determined. Time required to analyze each tree core was recorded by using checking the clock at the start and end of each workday. The manual method took a total of 27.84 hours to complete the analysis process, including tree ring measurement and software processing. This traditional method requires a set-up of multiple specialized equipment and software, which contains the microscope, the unislide, and Measure J2x software. The total cost reached $3,702.99 when these required software and equipment were purchase between 2019–2020.

The semi-automatic relies on image analysis in specialized software based on scanned high-resolution images of the cores. The main cost is the flatbed Epson Perfection V850 Pro Scanner, $999.00 as purchased in 2019. The image analysis software includes the CDendro and CooRecorder programs (https://www.cybis.se/forfun/dendro/helpcoorecorder7/), which only cost $68 for a registered user license. Therefore, the total cost of the semi-automatic method is $1,067.00. The learning curve of this system was much shorter than that of the manual method, and the semi-automatic method took a total 21.69 hours to analyze the tree core samples.

The difference between the two methods was a time of 6.15 hours and a cost of $2,635.99, making the semi-automatic method a less costly and faster alternative to the manual method with little change in results. The time and cost of each method are broken down in Tables 3 and 4, respectively. The total time required to perform each method was estimated somewhat subjectively, but a significant shortened period is noticed when performing the semi-automatic work. The time required to analyze core samples in both methods declined as the study continued due to becoming more familiar with equipment and software.

Table 3. Total time required to measure the tree core samples using the manual and semi-automatic methods.

	Manual Method	**Semi-automatic Method**
Time (min) measuring cores	1,432.2	1,153.2
Time learning components and software (min)	238	148
Total time (min)	1,670.2	1,301.2
Total time (hr)	27.84	21.69

Table 4. Total cost breakdown of lab equipment and software required for the manual and semi-automatic methods.

Method	**Category**	**Item**	**Price**	**Total Cost (Software + Equipment)**
Manual	Software	MeasureJ2X	$180.00	
	Equipment	3.5X-90X Boom Stand Trinocular Zoom Stereo Microscope + 54 LED Light	$522.99	
	Equipment	Velmex Tree Ring Measurement System	$3,000.00	$3,702.99
Semi-automatic	Software	Cdendro + CooRecorder Individual user license	$68.00	
	Equipment	Epson Perfection V850 Pro Scanner	$999.00	$1,067.00

5.2 Timing of the Glacial Retreat

Crossdating Results

Crossdating tree cores ensures that samples are accurately dated to exact years by comparing the pattern of rings in each core to the rest of the cores. Of the 52 measured tree cores, only 48 of the cores were used for the correlation statistics. The four core samples from trees XTX010 and XTX017 were removed because of their poor correlation with the master chronology composited from the rest of the samples. A total of 5,623 tree ring measurements were recorded across all samples. The final series span from 1640 to 2019, ranging 380 years, with an average length of 117 years per core (Table 5). The series intercorrelation measures how well the tree core samples correlate with each other, and the mean series intercorrelation for this dataset is 0.4959. This indicates that the tree core samples are reliably crossdated and have been accurately dated. Figure 9 illustrates the strength of the intercorrelation between cores. Most segments across the series are well correlated, with only a few segments with potential dating errors. The autoregression coefficient (AR1) is an indicator of how much the previous year's growth is affecting the current year's growth. The AR1 was 0.7747, suggesting that there is a high autocorrelation or consistency in growth between consecutive years. The average gini coefficient was 0.2054, indicating that the trees have similar responses to their environment. Detailed statistics derived from xDateR program are presented in Table 5.

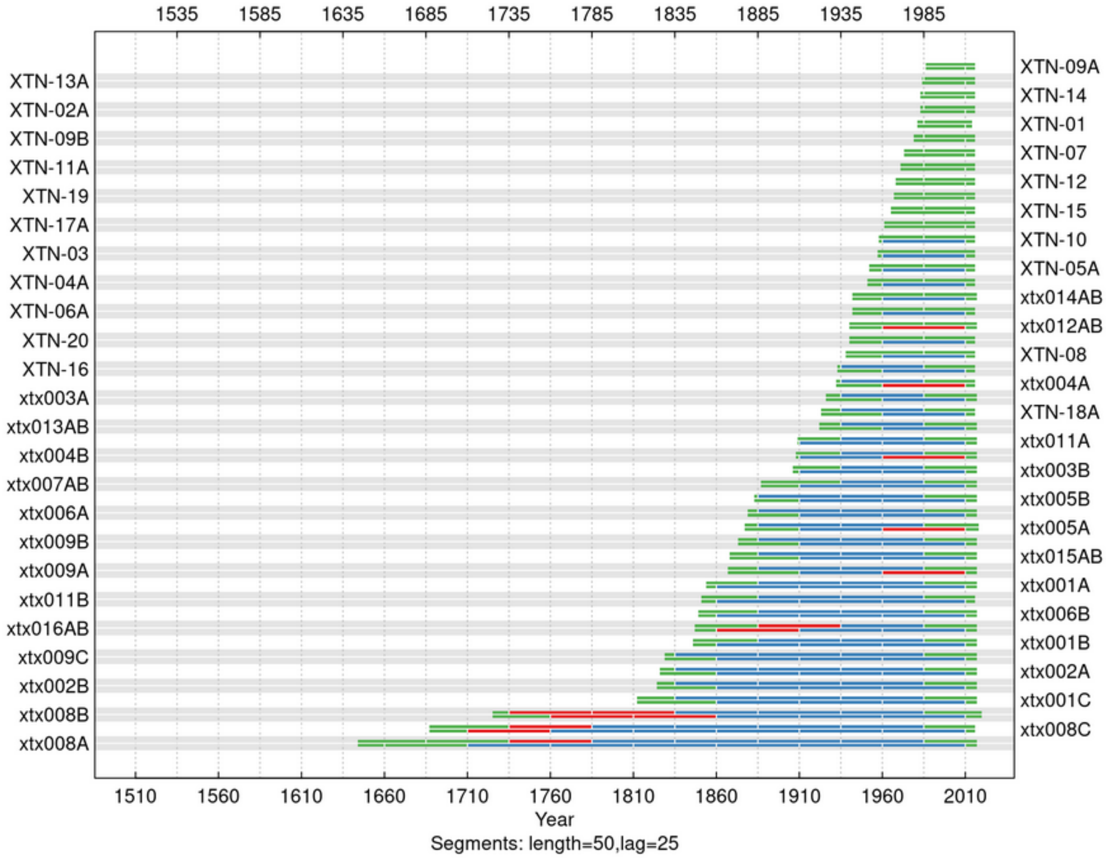

Figure 9: Segment graph depicting the 48 series that were crossdated. Correlations were calculated on overlapping segments; 50-year segments overlapping by 25 years. Each color illustrates the strength of the correlation between that segment and the master chronology. Blue: well correlated; Red: potential dating problems; Green: time periods that do not fully overlap and have not had a correlation calculated.

Table 5: Summary statistics of the crossdated samples, derived from xDateR program.

Number of dated series:	48
Number of measurements:	5,623
Avg series length:	117.1458
Range:	380
Span:	1640 – 2019
Mean (std dev) series intercorrelation:	0.4959 (0.1356)
Mean (std dev) AR1:	0.7747 (0.1526)

Germination Date and Ecesis Interval

The addition of the germination date and the ecesis interval to the tree age provides an estimate for the minimum age of the moraine. These measurements help bridge the gap between dates indicated by tree rings and the exposure of bare ground from glacial retreat. The mean height growth rate (cm/year) resulted 0.4371 cm/year, calculated from selected 2019 samples. This value was used in the formula, seen in Equation 1, to obtain the germination years for all the 2017 trees and the rest of 2019 trees, so that the true tree ages could be determined. The germination year for the 2019 samples was only calculated for trees that were sampled above 20 cm, because those taken below 20 cm, as indicated by Xu et al. (2012) would contain a pith that closely approximates the germination year. The tree age, germination year, and the ecesis interval (EI) can be seen in Table 6. The oldest tree sampled on the glacial moraine was tree XTX08, at 471 years old, germinating in 1554. With an EI of 7 years, minimum age of the moraine is 478 years old. This suggests the timing of the LIA glacial retreat is 1547.

Table 6: Age, germination year, and ecesis interval (EI) of the investigated trees. (Note: the order is presented ascendingly by Tree Age and the highlight marks the oldest tree.)

Tree ID	**Tree Age**	**Germination year**	**EI**
XTN13	92	1932	7
XTN02	104	1920	7
XTN01	107	1915	7
XTN14	120	1904	7
XTN09	129	1895	7
XTN12	130	1894	7
XTN11	150	1874	7
XTX12	156	1871	7
XTN15	166	1858	7
XTN07	171	1853	7
XTX14	175	1854	7
XTX13	186	1852	7
XTN17	188	1829	7
XTN10	193	1824	7
XTX04	213	1831	7
XTN19	219	1805	7
XTX15	224	1802	7
XTX07	225	1810	7
XTN16	234	1790	7
XTN06	235	1789	7
XTX05	239	1786	7
XTN03	242	1782	7
XTX03	253	1794	7
XTX11	256	1775	7
XTN08	257	1767	7
XTX09	259	1772	7
XTX06	261	1772	7
XTN20	263	1761	7
XTX01	264	1764	7
XTN04	268	1756	7
XTX16	270	1758	7
XTN05	305	1719	7
XTN18	305	1719	7
XTX02	307	1723	7
XTX08	471	1554	7

6. DISCUSSION

6.1 Comparison between the Manual and Semi-automatic Methods

Of the two chosen methods for tree ring measurement and crossdating, the semi-automatic method was more efficient than the manual method in terms of time and cost, while the dating results obtained between the two methods were not significantly different,. This might suggest that the semi-automatic method can be a viable alternative to the traditional method of analysis, with advantages of being faster and cheaper, without compromising results. Of note, however, was the 10-year difference obtained between the two methods when measuring tree cores from tree XTX08. This may have been due to mistakenly counting false or frost rings with one method and not the other or user error while processing and analyzing with the software.

The application of the photo scanner and CooRecorder software has become an accepted and common method in tree-ring studies in recent years (e.g. Bălut, et al., 2016; Schwalen, 2016; Maxwell and Larsson, 2021). One study similar to this study was conducted by Schwalen (2016), which compared the precision and efficiency of the traditional manual method to a similar image analysis method. This study found that both methods had room for human error during measurement (e.g. stage micrometer moved, poor image quality), and that the image analysis process took 1.4 times longer than the manual method. This finding is different from what was found in this project. Schwalen (2016), used a camera in addition to a scanner to obtain core images. Multiple images needed to be taken of a core when the camera was used. The camera images then had to be stitched together to make one cohesive image for analysis, which required an image stitching software called PTGui. This additional step may account for the difference in required semi-automatic analysis time between this project and the Schwalen study. The author states that, although this process took longer to perform, the actual time spent measuring the images was 7.5 minutes faster than using the manual method. This is an interesting note because most of the time spent analyzing the tree cores using the semi-automatic method in this study also went to preparing images for analysis. Another interesting note is that Schwalen (2016) also used CooRecorder for semi-automatic image analysis, stating that the CooRecorder program is cheaper than other software and is easier to learn than other programs. These reasons are very similar to why CooRecorder was chosen for this study in the first place.

6.2 Comparing the Little Ice Age timing with other regions

This study revealed that the oldest tree was 471 years old, germinating in 1554 on the newest set of moraines of the Xiata glacial valley. Accounting for the ecesis interval of 7 years, the minimum age of the moraine is then estimated to be 478 years old, inferring that the LIA glacial retreat occurred at least since 1547. This date is similar to those found by Yi et al. (2004), whose study dated two moraines in front of Glacier No. 1 to 1615 ±120 year and 1558 ± 120 years.

Through either field geomorphological interpretation or proxy-based timing constraints, studies across mountains in Northwest China suggested that there were three glacial advances during the LIA at approximately 1285, 1645, and 1805 (Chen, 1989; Solomina, Barry, and Bodyna, 2004; Yi et al., 2004; Chen, 2015; Li, 2016). In this study, a successional LIA retreat may have occurred around 1810, speculated from the age distribution of the trees sampled at the outer flank of the moraine (Figure 9 and Figure 10). With most trees dated after 1810, there may have existed successional moraines during the multiple cold periods of the LIA, but they are not distinguishable enough to observe the sequence in the field. If retreat had occurred at an earlier date, the surface of the ground would have been exposed for a longer period. This longer exposure would have allowed tree to colonize the surface sooner, meaning that the trees in this area would be much older.

Within the Tian Shan, lichenometry was used to conclude that the maximum glacier advances in the past millennium occurred in the Tian Shan valleys between the 1650s and the 1850s (Solomina, Barry, and Bodnya 2004). An earlier study by Chen (1989), also using lichenometry, dated three moraines in front of the Glacier No. 1 to approximately 1603 ± 20 years, 1842 ± 20 years, and 1936 ± 20 years. Yi et al. (2004) used Accelerator Mass Spectrometry (AMS) ^{14}C dating of inorganic carbonate coatings to obtain the ages of two moraines in the same area as Chen (1989). The ages Yi et al. (2004) recorded were 1615 ±120 years and 1585 ± 120 years, similar to the previous study. Work by Li (2016) used cosmogenic 10Be ages to date glacial moraines in the Urumqi River headwaters and in the Haxilegen Pass. The outermost moraines at both sites indicated a maximum LIA glacial advance around 1645 ± 100 years. Chen et al. (2015), using ^{10}Be, dated LIA moraines to approximately 1285 ± 300 years in the Karlik Range of the easternmost Tian Shan. These data across the Tian Shan suggest that there were three glacial advances during the LIA at approximately 1285, 1645, and 1805 (Chen, 1989; Solomina, Barry, and Bodyna, 2004; Yi et al., 2004; Chen, 2015; Li, 2016). The disparities between the furthest glacial extent within one range is not unique to the Tian Shan Mountains.

Sub-advances during the LIA period are discovered not only in northwestern

China but in other areas across the world. Within HMA, the Tibetan Plateau had periods of advance centered around 1585, 1770, and 1815, with minor retreats in between (Braüning, 2006). All three LIA cold periods in the Tian Shan occur just before the cold periods within the Tibetan Plateau. This may be because the Tian Shan lie at a higher latitude than the mountains of the Tibetan Plateau, experiencing colder temperatures in general. These dates are similar to other LIA cold periods in North and South America. Within Chile, there were cold periods between 1280-1460, 1560-1590, and 1850-1880 (Harrison and Winchester, 2000; Koch and Kilian, 2005). Two significant periods of cold in the Canadian Rockies occurred between 1700-1725 and 1825-1875. These periods of cold around the globe during the LIA appear to have occurred nearly synchronously.

In southern Tibet, through the use of tree rings, it was determined that the glacial maxima for the three glaciers studied occurred around 1760, 1807-1820, and 1580-1590 (Bräuning 2006). These glaciers began to retreat from their LIA maxima during the 1500s to early 1700s, and during the early 1400s to early 1500s, respectively (Bräuning, 2006; Xu and Yi, 2014; Yang et al., 2021). Tree ages determined by Xu and Yi (2014), in the Himalayas, Nyainqentanglha Shan, Tanggula Shan, Gongga Shan, Karakoram, Pamir Plateau, Tian Shan, and Qilian Shan, were significantly older, and it was determined that most of the glaciers had reached their LIA maxima by the 1300s.

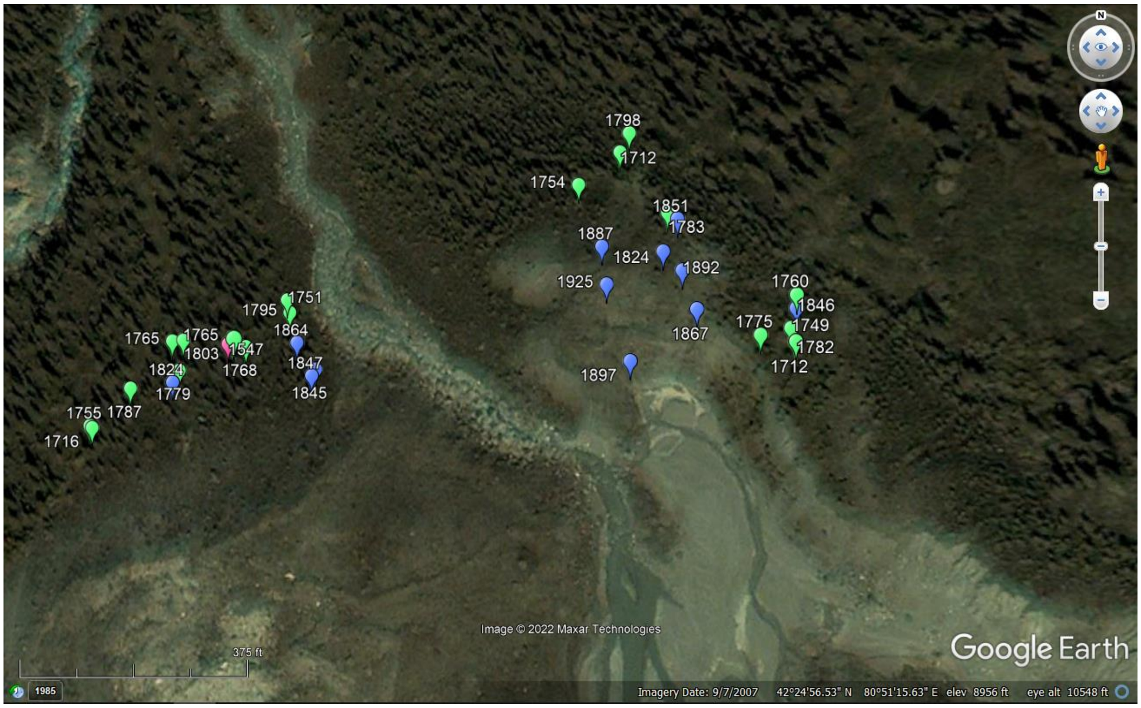

Figure 10. Age and location of each tree cored. The green markers indicate dates prior to 1810, the blue markers indicate dates after 1810, and the pink marker denotes the oldest tree.

6.3 Uncertainty, Limitations, and Future Directions

There are some sources of potential uncertainty in the data that can be derived from sampling, measurement, and estimation of landform ages, as well as environmental variables (e.g. precipitation, temperature, slope). For example, the summary statistics (Table 5) indicate that this site is relatively well dated, but there may be some stand dynamics effecting the area. Additionally, with a low gini coefficient (0.2054), there may be some type of localized disturbance that affects tree ring growth between trees. However, this disturbance may be attributed to the lack of comparative samples for more adequate crossdating of this section.

The high AR1 (0.7747) for the area suggests that the previous year's growth, has a significant effect on the current year's growth. For example, with a high AR1 value, if the tree ring from the previous year was wide the following year is likely to be wide as well. If the AR1 value is low, that would indicate that a year is not a significantly affected by the previous, so a year with a wide tree ring, would likely be followed by a narrower tree ring.

Each method of analysis was also potential for uncertainty. False rings and missing rings can be challenging and causing inaccuracy in dating. Another potential source of inaccuracy can come from the way in which tree rings are measured. Rings must be measured from the tangent on one ring to the next, and the point where that tangent is can vary between person to person.

A final point of uncertainty was the ecesis interval (EI). The EI was not able to be determined from satellite imagery as originally planned. Because of this an EI was used from the literature (Passmore et al., 2008), and although for the same tree species, each area has its own environmental conditions that can alter the length of the EI. Being able to determine a site-specific EI for the study area would offer greater insight into the area's glacial history.

There were several limitations in this project that had to be accounted for. Tree core collection itself was limited due to the remote location of the study site and rugged terrain. At the study site itself there were numerous trees that appeared to be old but presented with rotten trunks that prevented core sampling. Storing and transporting samples was difficult as well, due to the risk of damage or warping of the cores during transport.

Future dendroglaciological studies across the Tian Shan can offer greater insight into past climate. Hundreds of years of climate history can be reconstructed by using older trees within the Xiata Valley to correlate with glacial movement during the LIA.

This would help further the understanding of glacier-climate interrelationships. More sites throughout the CTS and other ranges of the Tian Shan need to be studied. If more moraines can be found that have been recolonized by trees, they can be dated using dendroglaciological techniques. This would provide a more complete picture of glacial fluctuations through the Tian Shan.

7. CONCLUSIONS

The primary purpose of this study was to approximate the timing of the Little Ice Age (LIA) glacier retreat in the central Tian Shan (CTS). This study found that the age of the LIA glacial retreat within the Xiata Valley was 1547. This period falls within known periods of cold during the LIA. This retreat occurred slightly before those seen in the Tibetan Plateau, possibly due to the Tian Shan's more northern climate. The years of retreat determined by this study, also fit in with LIA fluctuations on the global scale.

The secondary purpose of this study was to two compare two tree ring analysis methods for accuracy and efficiency. The manual method of measuring tree rings in a core sample was compared to a semi-automatic method of analysis. The semi-automatic was the more efficient analysis method, taking less time to date tree core samples, and was the more cost-effective of the two methods. The ages obtained between the two methods did not vary significantly, suggesting that the semi-automatic method could be a viable alternative method to the time-consuming and costly manual method.

The research done in this project leaves questions that could be answered through further study. As the EI could not be found with satellite imagery for this study, future work could be dedicated to further investigating the possibility of using remote sensing to determine the ecesis interval. This could be a supplemental method for determining the EI, especially in remote areas like the Tian Shan were there are knowledge gaps. Another avenue of investigation could be investigating temperature and precipitation trends in the study area to better understand localized factors that may have affected glacier retreat and tree ring growth.

As global climate change continues, is it important to better understand how glaciers fluctuate in response. Many towns and villages rely on glacial meltwater each year for agricultural and industrial use. With a warming climate, these meltwaters are appearing earlier and in stronger force. This can result in glacial lake outburst flood that can be devastating. The following months would be filled with water shortages and potentially drought. By having a more complete knowledge of past fluctuations and glacier response to climate predictive models can be enhanced.

REFERENCES

Anchukaitis, K.J., M. J. Taylor, J. Martin-Fernandez, D. Pons, M. Dell, C. Chopp, and E. J. Castellanos. 2013. Annual chronology and climate response in *Abies guatemalensis* Rehder (Pinaceae) in Central America. *The Holocene*, 23(2):270-277.

Applequist, M. B. 1958. A simple pith locator for use with off-center increment cores. *Journal of Forestry*, 56:141.

Bălut, M., F. Dinulică, I. Medrea, and A. M. I. C. Petriţan. 2016.A powerful and promising tool used in the tree ring measurements. *Revista de Silvicultură şi Cinegetică*, 21(38):27-33.

Bertrand, S., K. A. Hughen, F. Lamy, J.-B. W. Stuut, F. Torrejón, and C. B. Lange. 2012.
Precipitation as the main driver of Neoglacial fluctuations of Gualas glacier, Northern Patagonian Icefield. *Climate of the Past,* 8:519-534.

Bewley, J. D., and M. Black. 1994. Seeds. In *Seeds*, Boston, MA: Springer.

Bickerton, R. W., and J. A. Matthews. 1992. On the accuracy of lichenometric dates: an assessment based on the "Little Ice Age" moraine sequence of Nigardsbreen, southern Norway. *The Holocene,* 2(3):227-237.

Bishop, M. P., J. S. Kargel, H. K. Kieffer, D. J. MacKinnon, B. H. Raup, and J. F. Shroder Jr. 2017. Remote-sensing science and technology for studying glacier processes in high Asia. *Annals of Glaciology*, 31:164-170.

Biondi, F., L. P. Jamieson, S. Strachan, and J. Sibold. 2011. Dendroecological testing of the pyroclimatic hypothesis in the central Great Basin, Nevada, USA. *Ecosphere,* 2(1):1-20.

Bradley, R. S., and P. D. Jones. 1993. "Little Ice Age" summer temperature variations: Their nature and relevance to recent global warming trends. *The Holocene,* 3:367-376.

Bräuning, A. 2006. Tree-ring evidence of 'Little Ice Age' glacier advances in southern Tibet.*The Holocene*, 16(3): 369-380.

Bunn, A. G. 2010. Statistical and visual crossdating in R using the dplR library. *Dendrochronologia*, 28(4):251-258. doi: 10.1016/j.dendro.2009.12.001.

Bunn, A. G. 2008. A dendrochronology program library in R (dplR). *Dendrochronologia*, 26(2):115-124. doi: 10.1016/j.dendro.2008.01.002.

Burbank, D. W. 1981. A chronology of late Holocene glacier fluctuations on Mount Rainer, Washington. *Arctic and Alpine Research*, 13:369-386.

Butler, D. R. 1987. Teaching general principles and applications of dendrogeomorphology. *Journal of Geological Education*, 35:64-70.

Chen, J. 1989. Preliminary researches on lichenometric chronology of Holocene glacial fluctuations and on other topics in the headwater of Urumqi River, Tianshan Mountains. *Science in China Series B-Chemistry*, 32:1487–1500.

Chen, Y., Y. Li, Y. Wang, M. Zhang, Z. Cui, C. Yi, and G. Liu. 2015. Late Quaternary glacial history of the Karlik Range, easternmost Tian Shan, derived from ^{10}Be surface exposure and optically stimulated luminescence datings. *Quaternary Science Review*, 115:17–27.

Clements, F. E. 1904. Development and structure of vegetation. *Report on the Botanical Survey of Nebraska*, 7:50.

Duncan, R. P. 1989. An evaluation of errors in tree age estimates based on increment cores in Kahikatea (*Dacrycarpus darydioides*) New Zealand. *Natural Sciences*, 16(3):1-37.

Farinotti, D., W. W. Immerzeel, R. J. de Kok, D. J. Quincey, and A. Dehecq. 2020. Manifestations and mechanisms of the Karakoram glacier Anomaly. *Nature Geoscience*, 13:8-16.

Fritts, H. C. 1976. *Tree rings and climate*. New York City, NY: Academic Press Inc. Fujita, K., and Nuimura, T. 2011. Spatially heterogenous wastage of Himalayan glaciers. *Proceedings of the National Academy of Sciences*, 108(34):14011-14014. Doi: 10.1073/pnas.1106242108.

Gao, J., and Y. Liu. 2001. Applications of remote sensing, GIS and GPS in glaciology: a review. *Progress in Physical Geography: Earth and Environment*, 25(4):520-540.

Grissino-Mayer, H. D. 2003. A manual and tutorial for the proper use of an increment borer. *Tree-Ring Research*, 59(2): 63-79.

Grove, J. M. 2004. *Little Ice Ages: Ancient and Modern*, Vol. 1, 2. Routledge: London.

Harrison, S., and V. Winchester. 2000. Nineteenth- and twentieth-century glacier fluctuations and climatic implications in the Arco and Colonia Valleys, Hielo Patagónico Norte, Chile. *Arctic, Antarctic, and Alpine Research*, 32(1):55-63. doi:10.1080/5230430.2000.12003339.

Harrison, W. D. 2013. How do glaciers respond to climate? Perspectives from the simplest models. *Journal of Glaciology*, 59(217):949-960. Doi: 10.3189/2013JoG13J048.

Heusser, C. J. 1956. Post-glacial environments in the Canadian Rocky Mountains. *Ecological Monographs*, 26:253-302.

Hewitt, K. 2005. The Karakoram Anomaly? Glacier expansion and the "Elevation Effect," Karakoram Himalaya. *Mountain Research and Development*, 25(4):332-340.

Hochreuther, P., D. Loibl, J. Wernicke, H. Zhu, J. Grießinger, and A. Bräuning. 2015. Ages of major Little Ice Age glacier fluctuations on the southeast Tibetan Plateau derived from tree-ring-based moraine dating. *Palaeogeography, Palaeoclimatology, Palaeoecology*, 422:1-10.

Huo, Y., X. Gou, W. Liu, J. Li, F. Zhang, and K. Fang. 2017. Climate-growth relationships of Schrenk spruce (*Picea schrenkiana*) along an altitudinal gradient in the western Tianshan mountains, northwest China. *Trees*, 31:429-439.

Innes, J. L. 1985. Lichenometry. *Progress in Physical Geography: Earth and Environment*, 9(2):187-254.

Intergovernmental Panel on Climate Change. 2021. Summary for policymakers. In *Climate change 2021: The physical science basis*. Contribution of Working Group I to the Sixth Assessment Report of the Intergovernmental Panel on Climate Change, ed. Masson- Delmotte, V., P. Zhai, A. Pirani, S. L. Connors, C. Péan, S. Berger, N. Caud, Y. Chen, L. Goldfarb, M. I. Gomis, M. Huang, K. Leitzell, E. Lonnoy, J. B. R. Matthews, T. K. Maycock, T. Waterfield, O. Yelekçi, R. Yu and B. Zhou, Cambridge, England: Cambridge University Press.

Intergovernmental Panel on Climate Change. 2013. Summary for policymakers. In *Climate change 2013: The physical science base*. Contribution of Working Group I to the Fifth Assessment Report of the Intergovernmental Panel on Climate Change, ed. Church, J. A., P. U. Clark, A. Cazenave, J. M. Gregory, S. Jevrejeva, A. Levermann, M. A. Merrifield, G. A. Milne, R. S. Nermen, P. D. Nunn, A. J. Payne, W. T. Pfeffer, D. Stammer, and A. S. Unnikrishnan, England: Cambridge University Press.

Intergovernmental Panel on Climate Change. 2001. Summary for policymakers. In *TAR climate change 2001: The scientific basis*. Contribution of Working Group I to the Third Assessment Report of the Intergovernmental Panel on Climate Change, ed. Daniel L. Albritton, Myles R. Allen, Alfons P. M. Baede, John A. Church, Uüich Cubasch, Dai Xiaosu, Ding Yihui, Dieter H. Ehhalt, Christopher K. Folland, Filippo Giorgi, Jonathan M. Gregory, David J. Griggs, Jim M. Haywood, Bruce Hewitson, John T. Houghton, Joanna I. House, Michael Hulme, Ivar Isaksen, Victor J. Jaramillo, Achuthan Jayaraman, Catherine A. Johnson, Fortunat Joos, Sylvie Joussaume, Thomas Karl, David J. Karoly, Haroon S. Kheshgi, Corrine Le Quéré, Kathy Maskell, Luis J. Mata, Bryant J. McAvaney, Mack McFarland, Linda O. Mearns, Gerald A. Meehl, L. Gylvan Meira- Filho, Valentin P. Meleshko, John F. B. Mitchell, Berrien Moore, Richard K. Mugara, Maria Noguer, Buruhani S. Nyenzi, Michael Oppenheimer, Joyce E. Penner, Steven Pollonais, Michael Prather, I. Colin Prentice, Venkatchalam Ramaswamy, Armando Ramirez-Rojas, Sarah C. B. Raper, M. Jim Salinger, Robert J. Scholes, Susan Solomon, Thomas F. Stocker, John M. R. Stone, Ronald J. Stouffer, Kevin E. Trenberth, Ming- Xing Wang, Robert T. Watson, Kok S. Yap, John Zillman, Cmabridge, England: Cambridge University Press.

Jolivet, M., S. Dominquez, J. Charreau, Y. Chen, Y. Li, and Q. Wang. 2010. Mesozoic and Cenozoic tectonic history of the central Chinese Tian Shan: Reactivated tectonic structures and active deformation. *Tectonics*, 29(6):TC6019.

Kaennel, M., and F. H. Schweingruber. 1995. *Multilingual glossary of dendrochronology: Terms and definitions in English, German, French, Spanish, Italian, Portuguese, and Russian*.
Berne, Stuttgart, Vienna, Haupt: Birmensdorf, Swiss Federal Institute for Forest, Snow and Landscape Research.

Karlén, W. 1984. Dendrochronology, mass balance and glacier front fluctuations in northern Sweden. In *Climatic changes on a yearly to millennial basis*, ed. N.-A. Möerner and W. Karlén, 263-271. Dordrecht, Netherlands: D. Reidel Publishing Company.

Koch, J. 2009. Improving age estimates for late Holocene glacial landforms using dendrochronology – Some examples from Garibaldi Provincial Park, British Columbia. *Quaternary Geochronology*, 4(2):130-139. doi:10.1016/j.quageo.2008.11.002.

Koch, J., and R. Kilian. 2005. 'Little Ice Age' glacier fluctuations, Gran Campo Nevado, southernmost Chile. *The Holocene*, 15(1):20-28. doi:10.1191/0959683605hl780rp.

Kong, P., Fink, D., C. Na, F. Haung. 2009. Late quaternary glaciation of the Tianshan, Central Asia, using cosmogenic 10Be surface exposure dating. *Quaternary Research*, 72(2):229-233.

Kurtz, D., and E. Baker. 2016. 200 years of terminus retreat at Exit Glacier 1815-2015. NPS/KEFJ/NRR-2016/1341, National Park Service, Seward, Alaska, USA.

Lawrence, D. B. 1946. The technique of dating recent prehistoric glacial fluctuations from tree data. *Mazama*, 28:27-59.

Lewis, D. H., and D. J. Smith. 2004. Little Ice Age glacial activity in Strathcona Provincial Park, Vancouver Island, British Columbia, Canada. *Canadian Journal of Earth Science*, 41:285-297. doi:10.1139/E03-102.

Lewis, H. C. 1884. *Report on the Terminal Moraine in Pennsylvania and Western New York*. Vol 64. Harrisburg, PA: Board of Commissioners for the Second Geological Survey.

Li, J., Z. Li, J. Zhu, Z. Li, B. Xu, Q. Wang, C. Huang, and J. Hu. 2017. Early 21st century glacier thickness changes in the Central Tian Shan. *Remote Sensing of Environment*, 192:12-29.

Li, Y., G. Liu, P. Kong, J. Harbor, Y. Chen, and M. Caffee. 2011. Cosmogenic nuclide constraints on glacial chronology in the source area of the Urumqi River, Tian Shan, China.

Li, Y., G. Liu, Y. Chen, Y. Li, J. Harbor, A. P. Stroeven, M. Caffee, M. Zhang, C. Li, and X. Cui. 2014 Timing and extent of Quaternary glaciations in the Tianger Range, eastern Tian Shan, China, investigated using ^{10}Be surface exposure dating. *Quaternary Science Reviews*, 98:7-23.

Li, Y., Y. Li., J. Harbor, G. Liu, C. Yi., and M. W. Caffee. 2016. Cosmogenic ^{10}Be constraints on Little Ice Age glacial advances in the eastern Tian Shan, China.

Li, Y., and P. Fu. 2019. Mapping the Late-Holocene glacial geomorphology and glacier surface types on the Mt. Harajoriha, Central Tian Shan. *International Journal of Geosciences*, 10:669-688.

Libby, W. F. 1963. The accuracy of radiocarbon dates. *Antiquity*, 37(147):213-219.

Luckman, B. H. 2000. The Little Ice Age in the Canadian Rockies. *Geomorphology*, 32:357-384.

Luckman, B. H. 1998. Dendroglaciologie dans les Rocheuses du Canada. *Géographie physique et Quaternaire*, 52:139-151.

Luckman, B.H. 1994. Glacier fluctuation and tree-ring records for the last millennium in the Canadian Rockies. *Quaternary Science Reviews*, 12:441-450.

Luckman, B. H. 1988. Dating the moraines and recession of Athabasca and Dome Glaciers, Alberta, Canada. *Arctic and Alpine Research*, 20:40-54.

Luckman, B.H., and G. D. Osborn. 1979. Holocene glacier fluctuations in the middle Canadian Rocky Mountains. *Quaternary Research*, 11:52-77.

Lutz, H. J., 1930. Observations on the invasion of newly formed glacial moraines by trees. *Ecology*, 11:535-567.

Mann, M. E. 2002. *Little Ice Age*. Vol 1 of *The Earth System: physical and chemical dimensions of global environmental change*. Chichester, United Kingdom: John Wiley & Sons, Ltd.

Mann, M. E., R. S. Bradley, and M. K. Hughes. 1999. Northern hemisphere temperatures during the past millennium: Inferences, uncertainties, and limitations. *Geophysical Research Letters*, 26:759-762.

Matthes, F. 1939. Report of committee on glaciers. *Transactions American Geophysical Union*, 20:518-535.

Matthews, J. A., and K. R. Briffa. 2005. The 'Little Ice Age': Re-evaluation of an evolving concept. *Geografiska Annaler*, 87A(1):17-36.

Maurer, J. M., J. M. Schaefer, S. Rupper, and A. Corley. 2019. Acceleration of ice loss across the Himalayas over the past 40 years. *Science Advances*, 5:1-12.

Maxwell, R. S., and L. Larsson. 2021. Measuring tree-ring widths using the CooRecorder software application. *Dendrochronologia*, 67.

McCarthy, D. P., and B. H. Luckman. 1993. Estimating ecesis for tree-ring dating of moraines: a comparative study from the Canadian Cordillera. *Arctic and Alpine Research*, 25:63-68.

McCarthy, J. M., B. H. Luckman, and P. E. Kelly. 1991. Sampling height error correction for spruce seedlings in glacial forefields, Canadian Cordillera. *Arctic and Alpine Research*, 23:451-455.

Mercer, J. H., and M. P. Oscar. 1977. Radiocarbon dating of the last glaciation in Peru. *Geology*, 5(10):600-604.

Miller, J. D., W. W. Immerzeel, and G. Rees. 2012. Climate change impacts on glacier hydrology and river discharge in the Hindu Kush-Himalayas. *Mountain Research and Development*, 32(4):461-467.

National Aeronautics and Space Administration. 2021. Earth observatory glossary. https://earthobservatory.nasa.gov/glossary/l/n (accessed June 15, 2021).

Oerlemans, J., and J. P. F. Fortuin. 1992. Sensitivity of glaciers and small ice caps to greenhouse warming. *Science*, 258:115-117.

Oliver, C. D., A. B. Adams, and R. J. Zasoski. 1985. Disturbance and forest development in a recently deglaciated valley in northwestern Cascade Range of Washington, USA. *Canadian Journal of Forest Research*, 15:221-232.

Osborn, G., B. Menounos, J. Koch, J. J. Clague, and V. Wallis. 2007. Multi-proxy record of Holocene glacial history of the Spearhead and Fitzsimmons ranges, southern Coast Mountains, British Columbia. *Quaternary Science Reviews*, 26:479-493.

Osborn, G., D. McCarthy, A. LaBrie, and R. Burke. 2015. Lichenometric dating: Science or pseudo-science? *Quaternary Research*, 83(1):1-12.

Palmer, W. H., and A. K. Miller. 1961. Botanical evidence for the recession of a glacier. *Oikos*, 12:75-89.

Putkonen, J., and T. Swanson. 2003. Accuracy of cosmogenic ages for moraines. *Quaternary Research*, 59(2):255-261.

Qian, W., and Y. Zhu. 2002. Little Ice Age climate near Beijing, China, inferred from historical and stalagmite records. *Quaternary Research*, 57:109-119.

Racoviteanu, A. E., M. W. Williams, and R. G. Barry. 2008. Optical remote sensing of glacier characteristics: A review with focus on the Himalaya. *Sensors*, 8(5):3355-3383.

Rankl, M., C. Kienholz, and M. Braun. 2014. Glacier changes in the Karakoram region mapped by multimission satellite imagery. *Cryosphere*, 8:977-989.

Roe, G. H., M. B. Baker, and F. Herla. 2017. Centennial glacier retreat as categorical evidence of regional climate change. *Nature Geoscience*, 10:95-99.

Schickhoff, U., R. B. Singh, and S. Mal. 2016. Climate change and dynamics of glaciers and vegetation in the Himalaya: An overview. In *Climate Change, Glacier Response, and Vegetation Dynamics in the Himalaya*, ed. R. Singh, U. Schickhoff, and S. Mal, 1-26. Switzerland: Springer, Cham.

Schomacker, A. 2011. Moraine. In *Encyclopedia of Snow, Ice, and Glaciers, Encyclopedia of earth Sciences Series*, ed. V. P. Singh, Singh, P., and U. K. Haritashya. Dordrecht, Holland: Springer.

Schwalen, D. 2016. A comparison of chronology development methods in dendrochronology.

Schweingruber, F. H. 1988. *Tree Rings and Applications of Dendrochronology*. Dordrecht, Holland: Kluwer Academic Publishers.

Shackleton, N. J., and N. D. Opdyke. 1977. Oxygen isotope and palaeomagnetic evidence for early Northern Hemisphere glaciation. *Nature*, 270:216-219.

Shean, D. E., S, Bhushan, P. Montesano, D. R. Rounce, A. Arendt, and B. Osmanoglu. 2020. A systematic, regional, assessment of High Mountain Asia glacier mass balance. *Frontiers in Earth Science*, 7(363):1-19. Doi: 10.3389/feart.2016.00363.

Sherzer, W. H. 1905. Glacial studies in the Canadian Rockies and the Selkirks. *Smithsonian Miscellaneous Collections*, 47:453-496.

Sigafoos, R. S., and E. L. Hendricks. 1969. The time interval between stabilization of alpine glacial deposits and establishment of tree seedlings. *U.S. Geological Survey Professional Paper*, 650-B:B89-B93.

Sigdel, S. R., H. Zhang, H. Zhu, S. Muhammad, and E. Liang. 2020. Retreating glacier and advancing forest over the past 200 years in the central Himalayas. *Journal of Geophysical Research: Biosciences*, 125:1-14.

Smith, D. J., and Laroque, C. P. 1996. Dendroglaciological dating of a Little Ice Age glacial advance at Moving Glacier, Vancouver Island, British Columbia. *Geographie Physique et Quaternaire*, 50:47-55.

Smith, D. J., D. P. McCarthy, and M. E. Colenutt. 1995. Little Ice Age glacial activity in Peter Lougheed and Elk Lakes provincial parks, Canadian Rocky Mountains. *Canadian Journal of Earth Sciences*, 32:579-589.

Smith, D. J., and D. Lewis. 2007. Dendrochronology. In *Encyclopedia of Quaternary Science,* ed. S. A. Elias, 459-465. Oxford, England: Elsevier.

Solenn, N. 2008. Météo Climat for Tian Shan. http://meteo-climat-bzh.dyndns.org/station- 1933.php (accessed February 6, 2022).

Solomina O., R. Barry, and M. Bodnya. 2004. The retreat of Tien Shan glaciers (Kyrgyzstan) since the Little Ice Age estimated from aerial photographs, lichenometric and historical data. *Geografiska Annaler Series A: Physical Geography*, 86(2):205-215.

Solomina, O. N., O. S. Savoskul, and A. E. Cherkinsky. 1994. Glacier variations, mudflow activity and landscape development in the Aksay Valley (Tian Shan) during the late Holocene. *The Holocene*, 4(1):25-31.

Speer, J. H. 2010. *Fundamentals of Tree-Ring Research*. Tucson, AZ: University of Arizona Press.

Stokes, M. A., and T. L. Smiley. 1968. *An introduction to tree-ring dating*. Tucson, AZ: The University of Arizona Press.

Stoller-Conrad, J. 2017. Tree rings provide snapshots of Earth's past climate. https://climate.nasa.gov/news/2540/tree-rings-provide-snapshots-of-earths-past-climate/ (accessed March 7, 2022).

Telewski, F. W. 1993. Determining the germination date of woody plants: A proposed method for location root/shoot interface. *Tree0Ring Bulletin*, 53:13-16.

Telewski, F. W., and A. M. Lynch. 1991. Measuring growth and development of stems. In *Techniques and Approaches in Forest Tree Ecophysiology*, ed. J. P. Lassoie and T. M. Hinckley, 503-555. Boca Raton, FL: CRC Press.

Warren, C. R., and D. E. Sugden. 1993. The Patagonian Icefields: A Glaciological Review. *Arctic and Alpine Research*, 25(4):316.

Wang, S., M. Zhang, Z. Li, F. Wang, H. Li, Y. Li, and X. Huang. 2011. Glacier area variation and climate change in the Chinese Tianshan Mountains since 1960. *Journal of Geographical Sciences*, 21(2):263-273.

Wang, H., Y. Chan, Z. Chen, and W. Li. 2013 Changes in annual and seasonal temperature extremes in the arid region of China, 1960-2010. *Natural Hazards*, 65:1913-1930.

Wang, X., Y. Ding, S. Liu, L. Jiang, K. Wu, Z. Jiang, and W. Guo. 2013. Changes of glacial lakes and implications in Tian Shan, central Asia, based on remote sensing data from 1990 to 2010. *Environmental Research Letters*, 8:1-11.

Wiles, G. C., A. Post, E. H. Muller, and B. F. Molnia. 1999. Dendrochronology and late Holocene history of Bering Piedmont Glacier, Alaska. *Quaternary Research*, 52:185-195.

Xu, M., S. Kang, H. Wu, and X. Yuan. 2018. Detection of spatio-temporal variability of air temperature and precipitation on long-term meteorological station observations over Tianshan Mountains, Central Asia. *Atmospheric Research*, 203:141-163.

Xu X., and C. Yi. 2014. Little Ice Age on the Tibetan Plateau and its bordering mountains: Evidence from moraine chronologies. *Global and Planetary Change*, 116:41-53

Xu, P., H. Zhu, X. Shao, and Z. Yin, 2012. Tree ring-dated fluctuation history of Midui glacier since the little ice age in the southeastern Tibetan plateau. *Science China Earth Sciences*, 55(4):521-529.

Yang, D., F. Yang, Z. Niu, F. Shi, and N. Wang. 2021. Tree ring evidence of the retreat history of the Zepu glacier on the southern Tibetan Plateau since the Little Ice Age. *Quaternary International*, 604:60-67.

Yi, B., D. Yang, K. Jiao, T. Han, Z. Jin, H. Yan, and Z. Li. 2005. The Urumqi River source Glacier No. 1, Tianshan, China: Changes over the past 45 years. *Geophysical Research Letters*, 32(L21504):1-4.

Yi, C., K. Liu, Z. Cui, K. Jiao, T. Yao, and Y. He. 2004. AMS radiocarbon dating of late Quaternary glacial landforms, source of the Urumqi River, Tien Shan—a pilot study of ^{14}C dating on inorganic carbon. *Quaternary International*, 121:99–107.

Zhang, R., Y. Yuan, X. Gou, T. Zhang, C. Zou, C. Ji, Z, Fan, L. Qin, H. Shang, and X. Li. 2016. Intra-annual radial growth of Schrenk spruce (*Picea schrenkiana* Fisch. Et Mey) and its response to climate on the northern slopes on the Tianshan Mountains. *Dendrochronologia*, 40:36-42.

Zhang, T., Y. Yuan, Y. Liu, W. Wei, S. Yu, F. Chen. Z. Fan, H. Shang, R. Zhang, and L. Qin. 2013. A tree-ring based precipitation reconstruction for the Baluntai region on the southern slop of the central Tian Shan Mountains, China, since A.D. 1464. *Quaternary International*, 283:55-62.

Zhang, X., X. Shao, T. Wang. 2013 Regional climate characteristics in China during the Little Ice Age. *Journal of Nanjing University of Information Science and Technology: Natural Science Edition*, 4(1):317-325.

Zhu, H., X. Shao, H. Zhang, F. Asad, S. R. Sigdel, R. Huang, Y. Li, W. Liu, S. Muhammad, I. Hussain, J, Grießinger, and E. Liang. 2019. Trees record changes of the temperate glaciers on the Tibetan Plateau: Potential and uncertainty. *Global and Planetary Change*, 173:15-23.

Zhu, H., P. Xu, X. Shao, and H. Luo. 2013. Little Ice Age glacier fluctuations reconstructed for the southeastern Tibetan Plateau using tree rings. *Quaternary International*, 283:134-138.

Zhu, K. 1972. Preliminary study on climate changes in Chinese in recent 5000 years. *Science in China*, 16(2):226-256.